

A pipeline for fair comparison of graph neural networks in node classification tasks

Wentao Zhao^{a,b,*}, Dalin Zhou^c, Xinguo Qiu^a, Wei Jiang^a

^aCollege of Mechanical Engineering, Zhejiang University of Technology, Hangzhou, 310023, Zhejiang, China

^bSchool of Intelligent Transportation, Zhejiang Institute of Mechanical & Electrical Engineering, Hangzhou, 310053, Zhejiang, China

^cSchool of Computing, University of Portsmouth, Portsmouth, PO1 3HE, Hampshire, UK

Abstract

Graph neural networks (GNNs) have been investigated for potential applicability in multiple fields that employ graph data. However, there are no standard training settings to ensure fair comparisons among new methods, including different model architectures and data augmentation techniques. We introduce a standard, reproducible benchmark to which the same training settings can be applied for node classification. For this benchmark, we constructed 9 datasets, including both small- and medium-scale datasets from different fields, and 7 different models. We design a k-fold model assessment strategy for small datasets and a standard set of model training procedures for all datasets, enabling a standard experimental pipeline for GNNs to help ensure fair model architecture comparisons. We use node2vec and Laplacian eigenvectors to perform data augmentation to investigate how input features affect the performance of the models. We find topological information is important for node classification tasks. Increasing the number of model layers does not improve the performance except on the PATTERN and CLUSTER datasets, in which the graphs are not connected. Data augmentation is highly useful, especially using node2vec in the baseline, resulting in a substantial baseline performance improvement.

Keywords: graph neural network, node classification, deep learning, topological information

1. Introduction

Many classical models have been applied to perform deep learning studies on data analysis. The convolutional neural network (CNN) and recurrent neural network (RNN) have been used extensively in computer vision (CV) and natural language processing (NLP), respectively. However, when faced with graph-structured data, such as social networking service (SNS) datasets, knowledge graphs, molecular structures, and biological and financial networks, CNNs and RNNs are not easily applied due to the graph structure of the data [1]. To solve problems such as node classification [2] [3], graph classification [4] [5] [6], social recommendation [7] [8] and link prediction [9] [10], graph convolutional network (GCN) models [11], which exploit message-passing (or equivalently, various neighborhood functions) to precise high levels, have been proposed. More works have been done both optimizes performance of GCNs and solve real life problems. [12] optimizes GCNs from the feature importance perspective via statistical self-attention. [13] put forward a deep learning model, named InfGCN, to identify the most influential nodes in a complex network based on Graph Convolutional Networks. [14] use graph attention temporal convolutional networks to forecast short-term traffic speed. [15] propose a Multimodal Graph Convolutional Networks (MGCN) automatically filter high quality content from a large number of multimedia articles.

Thanks to the establishment of ImageNet [16], image classification in computer vision has undergone significant development, and many challenging and realistic benchmark datasets have been proposed that facilitate scalable, robust, and reproducible graph machine learning research. The Open Graph Benchmark [17] is one recent benchmark

*Corresponding author

Email address: zhaowentao163@163.com (Wentao Zhao)

¹<https://github.com/karl-zhao/benchmarking-gnns-pyg>

initiative whose goal is to represent large real-world datasets from various domains; it particularly emphasizes out-of-distribution rationalization performance through valid data splits. A steady trend toward improvement in model accuracy also has been demonstrated on various benchmarks. The accuracy of deep CNNs has developed steadily based on both model architecture improvements and data augmentation [18]. For graph neural networks (GNNs), [19] showed that different data splits lead to different model rankings on node classification tasks, and [20] proposed a fair performance comparison method for GNN architectures. Inspired by the above studies, we constructed a standardized and reproducible experimental environment in this study and used it to test how model architectures and data augmentation techniques impact node classification accuracy. The main contributions of our work are as follows.

- We collect a total of 9 datasets [21] [22] and 7 models that are widely used in various fields in the PyTorch [23] and PyTorch geometric [24] frameworks and use them to compare the expressive power of various model structures on different node classification tasks. For fair comparisons, we use 2 parameter budgets to ensure that the number of parameters and layers is roughly the same. To conduct further research, researchers can easily extend our framework by adding new models with different features and arbitrary datasets from their own experiments.
- We propose a method for fair comparison using the small datasets to evaluate model performance. The existing prior results show that applying small datasets with specific training/evaluation/test splits is unsuitable for making fair model comparisons. Therefore, we specify a 10-fold cross validation split for the small datasets instead of randomly splitting the data several times. We use this approach to build model assessment methods. We perform each experiment several times under the same training conditions to ensure fair comparisons.
- We test some input features to assess the expressive power of embedding by using node2vec and Laplacian vectors as data augmentation techniques to represent the node position and add to the input features. Using this approach, we can evaluate how the various input features affect the results.

The goal of this study is not to find the best-performing GNNs or to obtain the highest classification accuracy (which is computationally expensive) in the specific targets using an extensive hyperparameter grid search. Instead, our goal is to construct a standard benchmark for node classification and a uniform evaluation framework for GNNs. We use numerous GNNs to evaluate the power of the proposed architecture, and future researchers can easily use the framework to compare new proposed models using the existing architectures.

2. Training Procedures

A training process includes mainly datasets, models, and the strategy for updating model parameters. As we can see in the baseline training procedure in Figure 1, Algorithm 1 performs node classification with many graphs, while Algorithm 2 performs node classification for only one graph. For node classification, X is the embedding of the batch graph whose dimension is $N \times d$, where N denotes the number of nodes in the batch graphs, d denotes the dimension of each node, y is the node label, and the overall dimension is $N \times d$, where N denotes the number of nodes in the batch graphs and d denotes the dimension of the node label.

The difference between the 2 algorithms is that node classification from only one graph does not require a batch because for some node classification tasks, only one graph is available, and it is difficult to separate the nodes due to their relations. We emphasize that not all node classifications involve only one graph; some have multiple graphs and use minibatches during training. For these tasks, the algorithm process used is similar to Algorithm 1. For datasets that include more nodes and edges, it is easy to exceed the CUDA memory limitations when training models on a GPU; consequently, various methods have been proposed to solve the problems. One is to use a clustering algorithm to separate the graph into clusters and then randomly select some clusters for training, similar to algorithm 1 [25]. The other approach is to use sample subgraphs obtained via a random walk sampling algorithm [26].

2.1. Datasets

The datasets used in our experiments mainly stem from studies [22] [21] [27] that make benchmarks for different tasks. Here, we introduce the 9 datasets summarized in Table 1, including their split schemes, splits, features and

Algorithm 1: Training a neural network with the Adam optimizer for node classification

Input : Node embedding for every graph, initialize(net)

Output: Trained model

```

1 for epoch = 1,2,...,K do
2   for batch = 1,2,...,#graphs / b do
3     graphs ← uniformly random sample graphs;
4     X,y ← preprocess(graphs);
5     z ← forward(net,X);
6     l ← loss(z, y);
7     grad ← backward(l);
8     update(net,grad)
9   end
10 end

```

Algorithm 2: Training a neural network with the Adam optimizer for node classification

Input : Node embedding for every graph, initialize(net)

Output: Trained model

```

1 for epoch = 1,2,...,K do
2   X,y ← preprocess(graphs);
3   z ← forward(net,X);
4   l ← loss(z, y);
5   grad ← backward(l);
6   update(net,grad)
7 end

```

Figure 1: A baseline training procedure for node classification

Table 1: Summary of the datasets used in the experiments. A split strategy, the prediction task and the input features are described for each dataset. Additional details can be found in Section 2.1.

Name	#Tasks	Split Scheme	Split	Node Feat.	Edge Feat.	directed	Metric
cora	1	10-fold CV	08:01:01	✓	✗	✗	Acc
CiteSeer	1	10-fold CV	08:01:01	✓	✗	✗	Acc
PubMed	1	10-fold CV	08:01:01	✓	✗	✗	Acc
PATTERN	1	random	05:01:01	✓	✗	✗	Acc
CLUSTER	1	random	10:01:01	✓	✗	✗	Acc
Products	1	sales rank	196615:39323:2213091	✓	✗	✗	Acc
arXiv	1	time	90941:29799:48603	✓	✗	✓	Acc
MAG	1	time	629571:64879:41939	✓	✗	✓	Acc
Proteins	112	species	86619:21236:24679	✗	✓	✗	ROC-AUC

metrics. More details (such as the classes, domains, numbers of nodes and edges, and dimensions of the input features) are shown in Table A.6 (Appendix A).

Cora, CiteSeer and PubMed: For the node classification tasks, we first executed our experiment on three widely used benchmark datasets: Cora, CiteSeer and PubMed [27] [28], which are all citation networks.

Prediction task: For the Cora dataset, the task is to predict the subject of the paper (node) based on the surrounding node data and the graph structure. The different subjects are ‘Case Based’, ‘Genetic Algorithms’, ‘Neural Networks’, ‘Probabilistic Methods’, ‘Reinforcement Learning’, ‘Rule Learning’, and ‘Theory’. For the CiteSeer dataset, the task

is to predict which domain the paper (node) belongs to. All the papers are grouped into 6 classes: ‘Agents’, ‘AI’, ‘DB’, ‘IR’, ‘ML’ and ‘HCI’. The publications from the PubMed dataset pertaining to diabetes are classified into one of three classes: ‘Diabetes Mellitus, Experimental’, ‘Diabetes Mellitus Type 1’, or ‘Diabetes Mellitus Type 2’.

Dataset splitting: An earlier work [19] compared the performance of various GNNs on node classification tasks and found that choosing different training/validation/testing splits leads to different performance rankings. This result occurs primarily because the datasets used were too small to fully leverage the power of data-hungry GNNs. For fair comparisons, a 10-fold cross-validation split is used to train the models, similar to reference [20]. Ten sets of training, validation and testing data indices at a ratio of 8:1:1, respectively, are used to perform node classifications and calculate the test accuracy. Figure 2 reports the pseudocode of the entire process used to obtain the results of the classification accuracy, and the overall procedure is visually summarized in Figure A.4. Note that the model training processes are the same for Cora, CiteSeer and PubMed and that the datasets are represented later. We introduce the experimental setting in detail below.

PATTERN and **CLUSTER** are both artificially generated datasets generated with stochastic block models [29]. These datasets are widely used to model communities by modulating intra and extra community connections to control the difficulty of tasks in social networks, and they can be used for node classification tasks. **PATTERN** and **CLUSTER** contain a total of 14 K and 12 K graphs, respectively. The distribution of the number of nodes in these graphs is depicted in Figure A.5.

Prediction task: **PATTERN** [30] is used to recognize specific predetermined subgraphs. For all the data, a graph G is generated with 5 communities whose sizes are randomly selected between [5,35]. We then randomly generate 100 patterns P composed of 20 nodes. The node features for P and G are generated as a random signal with values of 0,1,2. The graph sizes are 44–195. The output node labels have a value of 1 if the node belongs to P and 0 if it belongs to G . **CLUSTER** is targeted at identifying community clusters. We generate 6 SBM clusters with randomly selected sizes in the range [5,35]. The graphs contain 40–190 nodes. Each node is embedded with a value from 0,1,2,...,6. If the value of the node is $a(a > 0)$, the node belongs to class $a - 1$, and if the value is 0, the node class is unknown. Only one labeled node is randomly assigned to each community, and most of the features are set to 0. When calculating accuracy, we use weighted accuracy w.r.t. the class sizes.

Dataset splitting: The **PATTERN** and **CLUSTER** datasets are both split randomly. The **PATTERN** dataset split includes 10,000 training, 2,000 validation, and 2,000 testing graphs, while the **CLUSTER** dataset is split into 10,000 training, 1,000 validation, and 1,000 testing graphs. We save the splits and subsequently use them to ensure fair comparisons. In addition to the artificially generated datasets, we import some datasets from the open graph benchmark dataset (OGB) [17]. The graphs all stem from real-world tasks. Unlike the datasets discussed above, these datasets include only one graph.

Products: The **Products** dataset is an undirected and unweighted graph. It is an Amazon product co-purchasing network [31]. The node features and the edges between 2 nodes are represented by a dimensionality-reduced bag-of-words of the product descriptions and the products that are purchased together, respectively, following [25].

Prediction task: The task is to predict which category the product belongs to. Forty-seven top-level categories are used as the target labels.

Dataset splitting: The previously used Cora, CiteSeer, and PubMed citation networks are typically split randomly; however, instead of performing a random split, [17] split the dataset by sales ranking. The top 8%, the next top 2% and the remainder of the records are used for training, validation and testing, respectively. Thus, as in real-world scenarios, we label the most popular products and leave the less popular products for validation and testing. This is a more realistic segmentation approach.

arXiv: arXiv is a directed graph that represents the citation network between all computer science (CS) arXiv papers [32]. The nodes represent an arXiv paper embedded with a 128-dimensional feature vector obtained by averaging the embeddings of the words in its title and abstract.

Prediction task: The task is to predict the subject areas to which an arXiv CS paper belongs (e.g., cs.AI, cs.LG, and cs.OS). The dataset includes forty labels that were manually determined by the paper’s authors and arXiv moderators.

Dataset splitting: We use a realistic data split based on the publication date of the papers to split this dataset; thus, papers published through 2017 are used for training, and papers published in 2018 and 2019 are used as validation and testing datasets, respectively.

MAG: MAG is a heterogeneous network composed of a subset of the Microsoft Academic Graph (MAG) [32]. It consists of 4 entity types: papers (736,839 nodes), authors (1,134,649 nodes), fields of study (59,965 nodes) and

Algorithm 3: Model Assessment(k -fold CV)

Input : Node embedding for graph \mathcal{D} , initialize(net)
Output: Test Acc.

- 1 Split \mathcal{D} into k folds F_1, \dots, F_k ;
- 2 **for** $i = 1, 2, \dots, k$ **do**
- 3 $train_k, valid_k, test_k \leftarrow (\cup_{j \neq i} F_j), F_i$;
- 4 **for** $z = 1, 2, \dots, R$ **do**
- 5 $model_r \leftarrow Train(train_k, valid_k)$;
- 6 $p_r \leftarrow Eval(model_k, test_k)$;
- 7 **end**
- 8 $perf_k \leftarrow \sum_{r=1}^R p_r / R$;
- 9 **end**
- 10 **return** $\sum_{i=1}^k perf_i / k$

Algorithm 4: Model Training

Input : $train_k, valid_k, initialize(net)$
Output: Trained model

- 1 **for** $epoch = 1, 2, \dots, N$ **do**
- 2 $model \leftarrow Train(train_k)$;
- 3 $lossval_n \leftarrow Eval(model, valid_k)$;
- 4 **while** $lossval_n > lossval_{n-1}$ **do**
- 5 $patience ++$;
- 6 **if** $patience \geq lr_schedule_patience$ **then**
- 7 $lr = lr \times 0.5$;
- 8 $patience = 0$;
- 9 **end**
- 10 **end**
- 11 **if** $lr \leq min_{lr}$ **or** $time > max_{time}$ **then**
- 12 $break$
- 13 **end**
- 14 **end**
- 15 **return** model

Figure 2: Pseudocode for model assessment (top) and model training (bottom). In Algorithm 3, ‘Train’ refers to Algorithm 4, whereas a strategy is introduced to train the models according to the results of the inference phases. The models are then used to test the classification accuracy in the $test_k$ part and obtain the p_r . We train the models and test them R times and obtain the average $perf_k$. Finally, the experiments are used in the k -fold CV, and the average results are obtained.

institutions (8,740 nodes). In addition, 4 types of directed relations connect 2 of the entity types. Each author is affiliated with an institution, an author writes a paper, the paper cites other papers, and each paper has a primary topic field of study. A 128-dimensional word2vec feature vector is used as the paper node embeddings. The other node types are not associated with the input node features.

Prediction task: The task is to predict the venue (conference or journal) at which each paper was presented. Based on the data, the papers could theoretically have been presented at any of 349 different venues, making the task a 349-class classification problem. To simplify the task, we consider only the paper nodes and the types of directed relations connecting 2 entity types, namely, a paper citing another paper, to transfer the task to be dealt with by an isomorphic graph.

Dataset splitting: Similar to arXiv data, we consider a realistic data split based on the paper publication dates. In practice, we always train on older existing papers and test on newer published papers. Finally, we used the papers

published through 2017 for training. The papers published in 2018 and 2019 are used as the validation and testing datasets, respectively.

Proteins: Proteins consist of undirected, weighted, and typed graphs where the nodes represent proteins, and the edges indicate different types of biologically meaningful associations between proteins [33] [34]. All the edges are embedded with 8-dimensional features. Each dimension represents the strength of a single association type and takes a value between 0 and 1. The dataset includes a total of 8 association types, constituting 8-dimensional features. In contrast to the other datasets, the proteins do not have node features; they possess only edge features—but there are more than 30 million edges. To better train the model using the input features, we use the averaged edge features of incoming edges as node features.

Prediction task: The task is to predict whether various protein functions are present. In total, there are 112 possible labels to predict. The result is measured by the average of the ROC-AUC scores across the 112 tasks.

Dataset splitting: We split the protein nodes according to the species from which the proteins come. This makes it possible to evaluate model generalizability across different species.

2.2. Embedded Information Regarding the Datasets

Using Laplacian eigenvectors as positional embeddings: For a graph, the positional features that represent each node are important, especially when working with graphs that exhibit symmetry in their structures, such as node or edge isomorphism [35] [36]. Laplacian eigenvectors [37] are a technique that embeds graphs into Euclidean space. The eigenvectors are used to build a meaningful local coordinate system that preserves the global graph structure. The eigenvectors are defined via factorization of the graph’s Laplacian matrix.

$$\Delta = \mathbf{I} - D^{-1/2}AD^{-1/2} = U^T \Lambda U \quad (1)$$

The Laplacian eigenvectors of a graph can be calculated by Laplace decomposition, where A is the $n \times n$ adjacency matrix, D is the degree matrix, Λ is the eigenvalue and U is the eigenvector. U is a type of positional encoding; the k -smallest nontrivial encoding is used as a supplement to the node embeddings to enrich the input node information. Laplacian eigenvectors are used to provide smooth encoding coordinates for neighboring nodes.

Node2vec [38]: In NLP tasks, word2vec [39] is a commonly used word embedding method that describes the cooccurrence relationships between words in sentence sequences in the corpus and then learns the vector representation of words. The idea behind node2vec is similar to word2vec; it uses the node co-occurrences in the graph to learn the vector representations of nodes. In contrast to deepwalk [8] or randomwalk to obtain the nearest neighbor sequence of vertices, node2vec uses a biased random walk. It is an unsupervised node embedding method.

2.3. Model Selection

To ensure fair model comparisons, a parameter budget for the models is controlled in our experiments. The pipeline of experiments is illustrated in Figure 3 for all GNNs. First, an embedding layer is used in the input layer to satisfy the input requirements of the GNN layers. GNN layers are then used in the $L \times GNN$ layers as well as the batch norm and activation function. Finally, MLP is used to embed the graph.

Most GNN implementations involve a GCN-Graph Convolutional Network [11], GAT-Graph Attention Network [40], GraphSAGE [41], GIN-Graph Isomorphism Network [42], MoNet-Gaussian Mixture Model Network [43], Residual Gated Graph Convolutional Network [44], and Gated Graph Convolutional Network [45]. All these model architectures are explained in Appendix B.

3. Experiments

3.1. Data Splitting and Model Assessment

On small datasets such as Cora, CiteSeer and PubMed, we use the k -fold cross-validation split for model assessment. As shown in Algorithm 3 (Figure 2), we first split the datasets into k folds ($k = 10$). Note that the class proportions are preserved in all the data splits (training, validation, and testing splits). All the data partitions are pre-processed; thus, the models are trained and evaluated on the same data splits. We train the models R times ($R = 3$) on each training and validation fold and obtain an average accuracy $perf_k$ for each fold. The average of the k folds is used

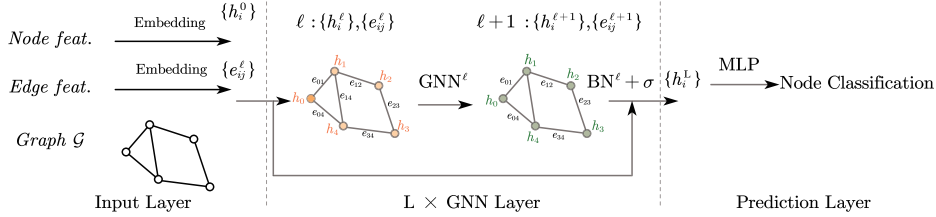


Figure 3: A standard experimental pipeline for GNNs that embeds the graph nodes and edges to dimensions of $N \times \text{hidden_dim}$ and $E \times \text{hidden_dim}$, respectively, and then uses them as input features with the *edge_index* in the input layer. L layers of the GNN layers are used with the batch norms, activation functions and residual connections. Finally, an MLP is used to embed the nodes with $N \times \text{hidden_dim}$ to $N \times \text{classes}$ to perform classification.

as the final accuracy result of the classification. Finally, we execute each model 4 times with different seeds and use the mean value as the final classification result. On the other datasets, the respective strategies for splitting the datasets are introduced above; each model is executed 4 times, and the mean accuracy is taken as the final classification result.

3.2. Training

The goal of this study is not to find an optimal set of hyperparameters to obtain the best model performance but rather to compare the power of models within a parameter budget. For the same datasets, we use the same hyperparameters to train the models for node classification. A budget of parameters—including different numbers of layers—is used to help ensure a fair model comparison; the details can be seen in the results. The model training process strategy is the same for all the datasets, and the value of N is set to 1,000 (Algorithm 4 in Figure 2). If the inference results $loss_{val_n}$ are not decreased $lr_schedule_patience$ times, the learning rate will decrease by half. We implement early stopping when $lr \leq min_{lr}$ or $time > max_{time}$. For the loss function, all use the CrossEntropyLoss except the proteins, which use the BCEWithLogitsLoss because of the special classified content. The Adam optimizer [46] for all models is used in the experiments, and the hyperparameters, e.g., initial learning rate, patience times, min_{lr} , and max_{lr} , are shown in the code.

4. Results and Discussion

We perform the experiments on 3 planetoid datasets, Cora, CiteSeer and PubMed. The model training and model assessment methods are shown in Section 3 (Experiments), and each dataset has 2 parameter budgets. Due to the different dimensions of the input features, different numbers of parameter budgets are used for each dataset. For Cora, CiteSeer and PubMed, 260k/460k, 550k/750k and 150k/350k parameters are used, respectively. The small parameter budget has 4 layers, while the larger budget has 16 layers. The experimental pipeline for GNNs is shown in Section 2.3(Model selection). Our goal is to conduct a fair comparison of the different model architectures on small datasets using the same settings.

Table 2 shows the results of our experiments. We find that for deeper layers, the results sometimes do not improve. As the model depth increases, GNNs tend to suffer performance degeneration. The main reasons for this phenomenon are overfitting, oversmoothing [47] and vanishing gradients. Importantly, for the Cora and CiteSeer datasets, all the GNNs clearly outperform the MLP. The results suggest that the GNNs can actually exploit the topological information of the graphs in the dataset. However, for PubMed, the power of the topological information of the graphs is inconspicuous. Due to the small datasets, the results are easily overfitted. Most GNNs reach the accuracy of the training dataset near 100%. For all the models, GIN with 16 layers performs best in 2 small datasets and performs well in the other small dataset. For the baseline, MLP, an overly parameterized baseline, is not able to overfit the training data completely, even worsening. The baseline results have a higher standard deviation than the GNNs. This shows the training instability of the MLP.

Table 3 shows the results on the PATTERN and CLUSTERZ datasets, which are widely used in social networks. Note that they are weighted accuracies w.r.t. the class sizes, and the same training hyperparameters are used during training for a fair comparison. For PATTERN and CLUSTER, 2 classes and 6 classes exist, respectively (see Table A.6,

Table 2: Performance on the Planetoid datasets with 10-fold cross-validation. All the experiments were executed 4 times using the same hyperparameters with different seeds, and the mean \pm standard deviation of the results was calculated. The highest value and good values are indicated in red and blue respectively.

dataset	Model	L	params	Train Acc.	Val Acc.	Test Acc.	Epoch
Cora	MLP	4	260167	90.873 \pm 5.5075	54.4803 \pm 2.4206	53.6274 \pm 2.8318	217.9 \pm 3.2939
		16	458311	46.8908 \pm 2.2576	39.1298 \pm 1.1797	38.2718 \pm 1.0889	222.8833 \pm 0.8813
	GCN	4	261191	99.9996 \pm 0.0008	85.4674 \pm 0.1454	84.9894 \pm 0.119	225.6583 \pm 0.9539
		16	462407	99.9604 \pm 0.0092	85.5166 \pm 0.2035	84.6536 \pm 0.191	226.55 \pm 1.9809
	GraphSage	4	263673	100.0 \pm 0.0	85.9472 \pm 0.2164	85.515 \pm 0.2481	216.2333 \pm 0.9416
		16	466625	100.0 \pm 0.0	86.3684 \pm 0.4295	85.6969 \pm 0.3015	211.2334 \pm 0.2108
	ResGatedGCN	4	264387	99.9996 \pm 0.0008	85.9225 \pm 0.4375	85.3889 \pm 0.6281	222.2583 \pm 0.9492
		16	467887	99.9973 \pm 0.0054	86.1562 \pm 0.2771	85.7521 \pm 0.3085	216.9083 \pm 1.113
	GatedGCN	4	268739	99.9642 \pm 0.017	86.3377 \pm 0.5164	86.2045 \pm 0.341	237.75 \pm 2.0314
		16	465219	98.1284 \pm 0.1248	85.8856 \pm 0.2054	84.8385 \pm 0.2387	382.7583 \pm 2.8856
	GAT	4	262215	99.9907 \pm 0.0045	85.5658 \pm 0.0714	85.1954 \pm 0.1021	215.825 \pm 0.5494
		16	466503	99.9569 \pm 0.0078	85.981 \pm 0.1752	85.1492 \pm 0.2009	213.5167 \pm 2.0943
	GIN	4	261069	100.0 \pm 0.0	87.0388 \pm 0.1481	86.7398 \pm 0.0972	214.0416 \pm 0.1642
		16	461176	99.9919 \pm 0.0051	87.0541 \pm 0.2471	87.0323 \pm 0.1584	225.1333 \pm 0.7488
	Monet	4	265080	100.0 \pm 0.0	85.6796 \pm 0.3681	85.4138 \pm 0.3714	233.1334 \pm 2.6961
		16	464012	100.0 \pm 0.0	85.6243 \pm 0.491	85.287 \pm 0.5702	229.3667 \pm 3.1476
CiteSeer	MLP	4	550694	98.1854 \pm 1.1199	56.1987 \pm 2.3063	55.3595 \pm 2.2809	212.0 \pm 0.9518
		16	748838	51.4018 \pm 1.2994	35.4454 \pm 0.6745	35.347 \pm 0.8122	222.675 \pm 1.5597
	GCN	4	551718	99.9471 \pm 0.0041	70.3678 \pm 0.045	70.3118 \pm 0.0943	214.325 \pm 0.7416
		16	752934	99.7125 \pm 0.0565	70.5005 \pm 0.2185	70.7902 \pm 0.196	207.1916 \pm 6.2345
	GraphSage	4	547381	99.9775 \pm 0.0	72.8328 \pm 0.0484	72.6895 \pm 0.1979	208.6083 \pm 0.25
		16	753812	99.9775 \pm 0.0	72.002 \pm 0.3888	71.9955 \pm 0.3202	201.7666 \pm 0.9031
	ResGatedGCN	4	549534	99.9775 \pm 0.0	72.7853 \pm 0.7475	72.662 \pm 0.7147	211.5666 \pm 0.6492
		16	758467	99.9775 \pm 0.0	72.5751 \pm 0.4462	72.5316 \pm 0.3692	205.7417 \pm 0.3304
	GatedGCN	4	549282	99.975 \pm 0.0051	73.1131 \pm 0.1474	72.3867 \pm 0.0525	221.5084 \pm 0.747
		16	753285	99.5845 \pm 0.0472	72.44 \pm 0.415	71.4648 \pm 0.2711	267.825 \pm 0.3696
	GAT	4	552742	99.9236 \pm 0.0076	70.4905 \pm 0.1094	70.9206 \pm 0.1353	206.3583 \pm 0.5209
		16	757030	99.7893 \pm 0.0195	70.7558 \pm 0.2116	71.091 \pm 0.1623	199.875 \pm 0.9472
	GIN	4	549232	99.9743 \pm 0.0016	73.3083 \pm 0.1784	73.9664 \pm 0.0609	206.0666 \pm 0.4422
		16	752038	99.964 \pm 0.0048	74.024 \pm 0.0876	74.5226 \pm 0.0924	210.4 \pm 0.2341
	Monet	4	552277	99.9775 \pm 0.0	70.7908 \pm 0.5502	70.6258 \pm 0.4377	218.1166 \pm 0.5815
		16	757010	99.9775 \pm 0.0	70.3879 \pm 0.8566	70.0163 \pm 0.9597	211.6 \pm 3.5057
PubMed	MLP	4	152533	93.4437 \pm 0.0901	87.1062 \pm 0.1012	87.4948 \pm 0.1509	364.7 \pm 4.791
		16	348336	75.1723 \pm 14.5209	71.9386 \pm 13.2933	72.1064 \pm 13.3417	372.7 \pm 80.8246
	GCN	4	145016	99.9174 \pm 0.0169	86.7661 \pm 0.0859	87.1989 \pm 0.0994	254.8334 \pm 2.3816
		16	352496	99.7014 \pm 0.112	86.052 \pm 0.0587	86.2949 \pm 0.0843	247.3 \pm 5.5586
	GraphSage	4	151422	99.3514 \pm 0.1177	86.341 \pm 0.1768	86.3776 \pm 0.1825	254.375 \pm 0.5725
		16	353523	99.7196 \pm 0.0908	86.0389 \pm 0.1124	86.0648 \pm 0.1761	253.0583 \pm 0.2807
	ResGatedGCN	4	152922	99.655 \pm 0.0777	86.4018 \pm 0.0764	86.7698 \pm 0.1167	256.6 \pm 1.4887
		16	350115	99.8654 \pm 0.0201	86.3926 \pm 0.1037	86.6744 \pm 0.1131	253.525 \pm 2.955
	GatedGCN	4	152048	96.0368 \pm 0.0436	88.7754 \pm 0.0517	88.9004 \pm 0.0808	313.7583 \pm 3.5866
		16	352204	85.993 \pm 0.7327	83.2542 \pm 0.3806	83.3017 \pm 0.4354	800.15 \pm 15.954
	GAT	4	142659	99.6538 \pm 0.0963	86.0334 \pm 0.0754	86.269 \pm 0.0885	258.9 \pm 0.9714
		16	346947	99.858 \pm 0.0691	85.9129 \pm 0.137	86.3206 \pm 0.0949	257.55 \pm 7.1129
	GIN	4	151651	98.5947 \pm 0.1044	86.989 \pm 0.0058	87.3379 \pm 0.0801	250.5834 \pm 1.9525
		16	350427	95.6608 \pm 0.0557	87.2767 \pm 0.0569	87.564 \pm 0.0555	281.9583 \pm 2.7497
	Monet	4	150764	99.996 \pm 0.0058	87.8376 \pm 0.214	88.0703 \pm 0.176	249.875 \pm 7.1111
		16	355469	99.9901 \pm 0.0067	87.412 \pm 0.1406	87.665 \pm 0.1235	236.9083 \pm 2.5436

Appendix A). From the baseline, MLP, in which the topological information of the graphs is not used in the models, there are only near 50% and 21% in the classification, just near-random guesses. Even when the layers become deeper, the results do not improve. All the GNNs except GatedGCN obtain better performance using the graphic entity. There is no overfitting in the models, and as the GNNs become deeper, the results have a large boost (except for GatedGCN, the results have a large variance when training 4 times, and when training in CLUSTER in 32 layers, the results obtain only 20.9217%, just near the baseline). This is especially true in CLUSTER.

Table 3: Performance on the SBM datasets for node classification. All the experiments were executed 4 times using the same hyperparameters with different seeds, and the mean \pm standard deviation of the results was calculated. **Red**: the best model, **Blue**: good models.

dataset	Model	L	params	Train Acc.	Val Acc.	Test Acc.	Epoch
PATTERN	MLP	4	105263	50.2716 \pm 0.0132	50.501 \pm 0.0	50.505 \pm 0.0	42.0 \pm 0.0
		16	506819	50.1219 \pm 0.1409	50.1904 \pm 0.2407	50.1817 \pm 0.2396	42.0 \pm 0.0
	GCN	4	100923	85.7572 \pm 0.038	85.479 \pm 0.0136	85.6062\pm0.037	81.0 \pm 6.8313
		16	500823	86.1307 \pm 0.0542	85.511 \pm 0.0607	85.6337\pm0.0443	67.25 \pm 3.4034
	GraphSage	4	106123	61.5527 \pm 0.0265	60.7374 \pm 0.0715	60.8821 \pm 0.0196	89.5 \pm 8.8129
		16	499887	63.8495 \pm 0.0858	62.8452 \pm 0.1194	62.7988 \pm 0.0528	92.75 \pm 11.7011
	ResGatedGCN	4	104003	84.7557 \pm 0.2293	84.7014 \pm 0.217	84.8624 \pm 0.2249	78.5 \pm 10.3441
		16	502223	86.3522 \pm 0.0901	85.4158 \pm 0.0652	85.6615\pm0.0625	63.0 \pm 10.1653
	GatedGCN	8	106644	58.8313 \pm 10.3866	58.8632 \pm 10.2657	58.8123 \pm 10.1709	62.25 \pm 18.3371
		32	503339	75.0544 \pm 16.285	75.1626 \pm 16.6456	75.2675 \pm 16.6143	56.5 \pm 6.8069
	GAT	4	99398	76.9263 \pm 2.0962	75.1299 \pm 2.1181	75.1354 \pm 2.2154	90.5 \pm 15.9269
		16	529806	93.371 \pm 0.0896	77.4805 \pm 0.3171	77.5739 \pm 0.234	52.5 \pm 0.5774
	GIN	4	100884	85.9095 \pm 0.0814	85.4469 \pm 0.0175	85.7046\pm0.042	88.0 \pm 11.431
		16	508574	85.6501 \pm 0.1001	85.2367 \pm 0.1151	85.4734\pm0.0702	73.25 \pm 11.529
	MoNet	4	107774	85.4196 \pm 0.2936	85.303 \pm 0.2262	85.4708\pm0.2121	94.75 \pm 23.4147
		16	528431	86.2097 \pm 0.1729	85.6004 \pm 0.0611	85.8494\pm0.0263	65.5 \pm 2.6458
CLUSTER	MLP	4	106015	20.9432 \pm 0.0016	20.9954 \pm 0.0045	20.937 \pm 0.0087	43.0 \pm 2.0
		16	507691	20.944 \pm 0.0048	20.9986 \pm 0.0018	20.9282 \pm 0.0038	68.75 \pm 11.1467
	GCN	4	101655	49.743 \pm 3.5857	49.365 \pm 3.2667	48.4645 \pm 3.5681	63.0 \pm 4.5461
		16	501687	72.5567 \pm 3.7478	67.4692 \pm 2.0717	67.6036 \pm 2.3658	76.0 \pm 11.7473
	GraphSage	4	106675	54.9171 \pm 0.1076	54.65 \pm 0.0487	54.4518 \pm 0.1309	72.75 \pm 1.7078
		16	500503	63.0462 \pm 0.0499	62.2744 \pm 0.1038	62.4846 \pm 0.0369	80.25 \pm 11.6154
	ResGatedGCN	4	104355	62.3735 \pm 0.882	61.5646 \pm 0.7769	61.3884 \pm 0.7836	106.0 \pm 21.8021
		16	502615	87.4099 \pm 0.9555	73.4934 \pm 0.1984	73.56\pm0.292	60.25 \pm 3.7749
	GatedGCN	8	107072	36.3052 \pm 8.6864	36.4263 \pm 8.6648	36.1752 \pm 8.6751	94.25 \pm 12.5797
		32	503911	20.9779 \pm 0.0587	20.9943 \pm 0.1439	20.9217 \pm 0.2132	45.25 \pm 2.2174
	GAT	4	100122	58.8198 \pm 0.2584	58.0899 \pm 0.1739	57.9182 \pm 0.2563	69.0 \pm 4.0825
		16	530690	79.1966 \pm 0.4774	70.9993 \pm 0.2952	71.0611\pm0.3584	70.5 \pm 9.3274
	GIN	4	103544	59.765 \pm 0.2432	58.397 \pm 0.1926	58.3287 \pm 0.1755	77.0 \pm 2.708
		16	517570	66.4919 \pm 1.2986	64.736 \pm 1.1545	64.612 \pm 1.184	80.25 \pm 3.8622
	MoNet	4	108178	59.4267 \pm 0.5389	58.8536 \pm 0.443	58.6417 \pm 0.5125	73.25 \pm 7.719
		16	528883	75.792 \pm 2.1493	72.7219 \pm 1.3878	72.8281\pm1.3572	68.5 \pm 5.3229

Unlike the datasets for node classification, which have only 1 graph, PATTERN and CLUSTER have 14k and 12k graphs, respectively. The task is to classify the nodes in each graph. It seems that for these tasks, oversmoothing is not a serious problem because not all the nodes are connected together. It can also be found in the results that the accuracy of the classification improves when the layers become deeper. MoNet with 16 layers achieves the best performance.

The OGBN dataset in Table 4 was collected entirely from the Open Graph Benchmark [17]. The recent minibatch-based GNNs are always used in OGBN because there is only 1 graph, and these graphs can easily exceed the available CUDA memory during training. Before training using the different model architectures, we first randomly sample the nodes within a graph and return their induced subgraph to separate the dataset for all the datasets except arXiv (for arXiv, when choosing the appropriate parameters, the CUDA memory is sufficient to address the full-batch version of GNNs).

We can find that both GNNs perform well on arXiv and MAG, which both come from academic graphs; however, because MAG includes more classes than arXiv, performing classification in MAG is more difficult. Among these 4 datasets, the models GAT and GCN perform well compared to the others, while GIN, which uses feature outputs from each layer of the network, performs the worst—even worse than the baseline in Products when using 16 layers. As the layers become deeper, the MLP degrades on all 4 datasets. It seems that for the baseline, a large parameter budget does not achieve better performance.

Numerous methods for data augmentation have been proposed in the image classification field that can increase the classification accuracy. Here, we adopt the Node2vec embeddings and Laplacian eigenvectors to investigate how the input features affect the accuracy (see Table 5). The object datasets, including arXiv and Products, are used to test how the input features affect accuracy with the MLP, GCN and GAT models. We use MLP as the baseline and include

Table 4: Performance on the OGBN datasets including arXiv, MAG, Products and Proteins. All the results were executed 4 times using the same hyperparameters with different seeds, and the mean \pm standard deviation of the results was calculated. The highest value and good values are indicated in red and blue, respectively.

dataset	Model	L	params	Train Acc.	Val Acc.	Test Acc.	Epoch
arxiv	MLP	4	87720	50.6525 \pm 6.5617	50.975 \pm 5.517	48.955 \pm 5.385	780.5 \pm 252.3496
		8	162796	40.6975 \pm 15.3877	38.8375 \pm 20.8671	37.17 \pm 20.946	772.5 \pm 453.0
	GCN	4	88744	78.2106 \pm 0.3849	72.286 \pm 0.1538	70.7924 \pm 0.0895	378.0 \pm 37.833
		8	155816	78.7612 \pm 0.3607	72.5478 \pm 0.1401	71.0301 \pm 0.1616	345.75 \pm 8.2614
	GraphSage	4	89435	72.9625 \pm 0.2958	70.24 \pm 0.1211	69.4425 \pm 0.137	437.75 \pm 34.2868
		8	162775	72.7775 \pm 0.3179	70.3625 \pm 0.0685	69.53 \pm 0.1344	440.75 \pm 39.3563
	ResGatedGCN	4	89754	74.535 \pm 0.5071	70.3825 \pm 0.2047	69.23 \pm 0.1192	450.5 \pm 54.9272
		8	163703	76.2275 \pm 0.9221	70.29 \pm 0.0707	69.23 \pm 0.1594	409.25 \pm 41.064
	GatedGCN	4	91129	69.135 \pm 0.8843	69.0125 \pm 0.5955	68.09 \pm 0.4032	780.0 \pm 285.7633
		8	163750	43.985 \pm 2.7618	48.415 \pm 3.8031	49.0325 \pm 4.1766	251.0 \pm 77.9359
	GAT	4	89768	75.9825 \pm 0.3882	72.0225 \pm 0.0866	70.6325 \pm 0.1895	416.0 \pm 31.0376
		8	157864	77.23 \pm 0.3995	72.18 \pm 0.0356	70.73 \pm 0.1512	411.25 \pm 33.9153
	GIN	4	91467	69.455 \pm 2.2286	68.3875 \pm 1.376	67.155 \pm 1.3146	851.0 \pm 166.4612
		8	161613	65.0475 \pm 2.5219	65.0525 \pm 1.9444	63.93 \pm 1.9648	536.5 \pm 138.9208
	MoNet	4	91182	77.5175 \pm 0.4129	71.8275 \pm 0.2398	70.4775 \pm 0.1473	397.5 \pm 24.4609
		8	161276	78.3625 \pm 0.4305	71.9175 \pm 0.1484	70.425 \pm 0.1586	336.75 \pm 18.2094
MAG	MLP	4	133669	24.31 \pm 0.3383	23.5375 \pm 0.2438	24.665 \pm 0.2271	261.5 \pm 46.6655
		16	334969	18.3025 \pm 9.3862	16.8075 \pm 9.8013	17.4 \pm 10.7431	624.25 \pm 231.9258
	GCN	4	128605	31.5311 \pm 0.3482	29.8406 \pm 0.2038	30.4275 \pm 0.1321	127.5 \pm 16.1348
		16	329821	34.7873 \pm 0.5253	30.6906 \pm 0.0944	31.1542 \pm 0.0975	390.5 \pm 49.4672
	GraphSage	4	129349	28.485 \pm 0.1666	27.31 \pm 0.2467	28.2925 \pm 0.2568	114.75 \pm 7.5443
		16	332545	28.5775 \pm 0.2125	27.64 \pm 0.2436	28.62 \pm 0.2839	119.25 \pm 18.0069
	GatedGCN	4	129701	29.1425 \pm 0.4208	28.22 \pm 0.2341	29.3275 \pm 0.1528	197.75 \pm 31.3409
		16	330749	25.9875 \pm 0.857	25.8925 \pm 0.6019	27.175 \pm 0.7212	284.5 \pm 38.3884
	ResGatedGCN	4	131173	28.7325 \pm 0.1996	27.4975 \pm 0.1682	28.3725 \pm 0.125	138.75 \pm 10.4363
		16	336093	31.71 \pm 0.3636	29.715 \pm 0.3519	30.3275 \pm 0.1674	479.75 \pm 80.4669
	GAT	4	129629	31.2425 \pm 0.1839	29.7675 \pm 0.0709	30.4825 \pm 0.1103	130.25 \pm 17.0563
		16	333917	31.8075 \pm 0.1438	30.085 \pm 0.1784	30.7625 \pm 0.2109	136.75 \pm 10.2103
	GIN	4	130339	29.4775 \pm 0.2406	28.4675 \pm 0.1592	29.3925 \pm 0.2492	188.5 \pm 12.6886
		16	347859	27.3575 \pm 0.5762	26.7225 \pm 0.5816	27.74 \pm 0.6294	185.75 \pm 24.0468
	MoNet	4	130077	30.715 \pm 0.5753	29.18 \pm 0.535	30.195 \pm 0.4355	162.75 \pm 24.4046
		16	332341	30.5675 \pm 0.5389	29.3075 \pm 0.4807	30.1025 \pm 0.2951	168.25 \pm 17.595
Products	MLP	4	89807	81.015 \pm 0.6601	73.88 \pm 0.2464	59.7325 \pm 0.0378	77.25 \pm 5.909
		16	300479	83.3975 \pm 1.3537	70.05 \pm 0.1252	56.0825 \pm 0.1723	78.75 \pm 6.8496
	GCN	4	90863	92.4537 \pm 0.0749	90.9016 \pm 0.1326	75.2748 \pm 0.1767	118.5 \pm 13.3292
		16	300299	92.6767 \pm 0.0047	91.1668 \pm 0.075	76.018 \pm 0.1216	108.75 \pm 2.5
	GraphSage	4	92559	85.3525 \pm 0.0171	84.34 \pm 0.0408	66.0675 \pm 0.0842	93.0 \pm 6.4807
		16	307467	85.3425 \pm 0.0479	84.4025 \pm 0.0978	66.5275 \pm 0.0597	80.5 \pm 9.5743
	ResGatedGCN	4	91145	89.225 \pm 0.1526	88.3125 \pm 0.1305	71.775 \pm 0.3205	154.25 \pm 17.4428
		16	305687	89.05 \pm 0.4778	88.2325 \pm 0.4013	71.7875 \pm 0.7053	121.25 \pm 22.8674
	GatedGCN	4	89309	87.8825 \pm 0.4618	86.865 \pm 0.4828	73.355 \pm 0.4754	78.75 \pm 10.2429
		16	308937	69.76 \pm 4.1891	70.64 \pm 3.6577	61.6875 \pm 2.0558	57.5 \pm 2.6458
	GAT	4	96879	91.595 \pm 0.0995	90.21 \pm 0.0408	76.43 \pm 0.1485	148.75 \pm 12.816
		16	291375	92.1325 \pm 0.096	90.7575 \pm 0.159	77.345 \pm 0.1382	147.25 \pm 11.2064
	GIN	4	92111	66.2325 \pm 7.2651	68.9875 \pm 5.5578	63.2525 \pm 3.1596	90.0 \pm 11.7473
		16	297655	16.5525 \pm 8.2426	22.86 \pm 8.8685	33.6475 \pm 5.7637	61.25 \pm 3.304
	MoNet	4	89719	91.93 \pm 0.2192	89.6875 \pm 0.1821	74.3725 \pm 0.0814	86.0 \pm 6.9762
		16	309599	92.9 \pm 0.4473	90.085 \pm 0.3639	75.19 \pm 0.0825	77.25 \pm 4.272
Proteins	MLP	4	89887	80.41 \pm 0.3601	75.8725 \pm 0.2874	70.535 \pm 0.2042	93.25 \pm 12.5266
		16	301357	75.225 \pm 0.3854	71.47 \pm 0.2145	66.985 \pm 0.324	89.5 \pm 9.5743
	GCN	4	90967	85.988 \pm 0.3475	82.4895 \pm 0.3126	77.9989 \pm 0.1991	68.25 \pm 3.2016
		16	301204	86.1752 \pm 0.411	83.0136 \pm 0.2979	76.4456 \pm 0.7319	71.25 \pm 12.842
	GraphSage	4	89978	76.8275 \pm 0.0457	69.5225 \pm 0.1848	68.71 \pm 0.0648	52.5 \pm 3.0
		16	304967	77.375 \pm 0.09	69.7525 \pm 0.1367	68.95 \pm 0.1465	57.0 \pm 3.9158
	ResGatedGCN	4	89509	84.87 \pm 0.5857	81.4275 \pm 0.6523	78.18 \pm 0.8586	55.25 \pm 7.932
		16	304132	87.635 \pm 0.2428	83.765 \pm 0.1287	79.7175 \pm 0.2037	229.75 \pm 17.1731
	GatedGCN	4	90803	72.0325 \pm 3.3052	65.6975 \pm 7.5995	62.4425 \pm 8.421	45.5 \pm 1.7321
		16	305897	58.11 \pm 4.0229	53.4275 \pm 4.686	53.7925 \pm 1.1951	54.5 \pm 3.3166
	GAT	4	93272	83.4925 \pm 0.6073	79.8625 \pm 0.5536	75.1025 \pm 1.388	46.25 \pm 3.2016
		16	323384	85.4675 \pm 0.4718	81.5425 \pm 0.4513	77.03 \pm 0.6224	45.5 \pm 2.3805
	GIN	4	90039	47.395 \pm 5.8131	46.1875 \pm 6.8098	47.26 \pm 5.1833	44.25 \pm 1.893
		16	299350	49.04 \pm 2.5863	49.12 \pm 2.7496	49.36 \pm 2.0184	46.5 \pm 1.7321
	MoNet	4	92704	82.8725 \pm 1.2751	79.7775 \pm 1.0561	74.8025 \pm 1.0658	45.75 \pm 2.5
		16	299019	83.3425 \pm 1.303	79.5875 \pm 1.3526	75.06 \pm 0.8849	49.25 \pm 9.9121

GCN and GAT because all these models perform well on these 2 tasks. MLP in particular achieves a substantial im-

Table 5: Performance on the OGBN datasets including arXiv and Products. All the experiments were executed 4 times using the same hyper-parameters with different seeds, and the mean \pm standard deviation of the results was calculated. The indicators that improved significantly are highlighted in red, while the merely improved indicators are highlighted in blue. Models with the suffix -pe used Laplacian eigenvectors as node positional encodings with a dimension of 64. Models with the suffix -ne used node2vec embeddings in the input features.

dataset	Model	L	params	Train Acc.	Val Acc.	Test Acc.	Epoch
arxiv	MLP	4	87720	50.6525 \pm 6.5617	50.975 \pm 5.517	48.955 \pm 5.385	780.5 \pm 252.3496
		8	162796	40.6975 \pm 15.3877	38.8375 \pm 20.8671	37.17 \pm 20.946	772.5 \pm 453.0
	MLP-pe	4	96040	36.5803 \pm 15.0763	34.8024 \pm 19.657	32.6374 \pm 19.626	776.25 \pm 445.5
		8	171376	25.7848 \pm 15.7575	18.1466 \pm 21.0376	16.5201 \pm 21.3166	253.25 \pm 289.8521
	MLP-ne	4	104104	72.4907 \pm 0.4172	69.8774 \pm 0.1538	68.879\pm0.1818	667.5 \pm 71.9838
		8	179692	70.3805 \pm 2.2619	65.8 \pm 1.2338	64.5999\pm0.9095	757.5 \pm 185.5344
	GCN	4	88744	78.2106 \pm 0.3849	72.286 \pm 0.1538	70.7924 \pm 0.0895	378.0 \pm 37.833
		8	155816	78.7612 \pm 0.3607	72.5478 \pm 0.1401	71.0301 \pm 0.1616	345.75 \pm 8.2614
	GCN-pe	4	97064	77.8769 \pm 0.3842	72.1467 \pm 0.1701	70.8665\pm0.1229	358.5 \pm 11.7898
		8	164136	78.9484 \pm 0.1457	72.4572 \pm 0.1321	70.9961 \pm 0.0608	336.25 \pm 14.3614
	GCN-ne	4	105128	78.8789 \pm 0.1964	73.1568 \pm 0.094	71.814\pm0.1	310.75 \pm 14.2916
		8	172200	79.5466 \pm 0.2921	73.0906 \pm 0.1756	71.7137\pm0.0579	306.25 \pm 16.2763
	GAT	4	89768	75.9825 \pm 0.3882	72.0225 \pm 0.0866	70.6325 \pm 0.1895	416.0 \pm 31.0376
		8	157864	77.23 \pm 0.3995	72.18 \pm 0.0356	70.73 \pm 0.1512	411.25 \pm 33.9153
	GAT-pe	4	98088	75.5853 \pm 0.5619	71.8078 \pm 0.1395	70.651\pm0.2231	387.0 \pm 24.3721
		8	166184	77.2756 \pm 0.7433	72.0561 \pm 0.0529	70.6772 \pm 0.0362	353.0 \pm 21.9089
	GAT-ne	4	106152	77.5594 \pm 0.4013	72.9874 \pm 0.1534	71.5666\pm0.0926	361.0 \pm 11.6333
		8	174248	78.0253 \pm 0.2107	72.7978 \pm 0.1711	71.2682\pm0.1982	322.25 \pm 3.304
Products	MLP	4	89807	81.015 \pm 0.6601	73.88 \pm 0.2464	59.7325 \pm 0.0378	77.25 \pm 5.909
		16	300479	83.3975 \pm 1.3537	70.05 \pm 0.1252	56.0825 \pm 0.1723	78.75 \pm 6.8496
	MLP-pe	4	98387	81.2832 \pm 0.3376	73.9917 \pm 0.262	59.7828\pm0.0457	80.25 \pm 4.272
		16	309059	83.1328 \pm 0.3495	69.9654 \pm 0.5337	55.8319 \pm 0.4602	78.5 \pm 5.1962
	MLP-ne	4	106703	93.7025 \pm 0.0996	89.2162 \pm 0.086	70.9476\pm0.3534	68.5 \pm 2.3805
		16	317375	92.9284 \pm 1.5731	87.5626 \pm 0.2582	66.9452\pm0.446	68.0 \pm 5.7155
	GCN	4	90863	92.4537 \pm 0.0749	90.9016 \pm 0.1326	75.2748 \pm 0.1767	118.5 \pm 13.3292
		16	300299	92.6767 \pm 0.0047	91.1668 \pm 0.075	76.018 \pm 0.1216	108.75 \pm 2.5
	GCN-pe	4	99443	92.4556 \pm 0.1256	90.8343 \pm 0.1218	75.3129\pm0.1286	127.5 \pm 13.0767
		16	308814	92.7685 \pm 0.1377	91.2646 \pm 0.1161	76.1586\pm0.1262	121.75 \pm 9.7767
	GCN-ne	4	107759	93.5741 \pm 0.1473	91.7135 \pm 0.0884	75.0002 \pm 0.3371	85.0 \pm 10.4243
		16	317067	93.6397 \pm 0.1337	91.772 \pm 0.0534	74.6966 \pm 0.2146	94.75 \pm 9.4296
	GAT	4	96879	91.595 \pm 0.0995	90.21 \pm 0.0408	76.43 \pm 0.1485	148.75 \pm 12.816
		16	291375	92.1325 \pm 0.096	90.7575 \pm 0.159	77.345 \pm 0.1382	147.25 \pm 11.2064
	GAT-pe	4	105719	91.5923 \pm 0.0928	90.3072 \pm 0.0941	76.4812\pm0.1802	156.75 \pm 16.5202
		16	299695	92.3608 \pm 0.0987	90.8387 \pm 0.1179	77.3693\pm0.3204	144.0 \pm 4.5461
	GAT-ne	4	114287	93.2509 \pm 0.1768	91.4738 \pm 0.0939	76.2792 \pm 0.2283	104.25 \pm 11.8708
		16	307759	93.4481 \pm 0.2017	91.6169 \pm 0.1513	76.259 \pm 0.3628	116.0 \pm 10.2307

provement on 2 of the datasets with the node embedding features. It appears that the node embedding well represents the topological information in the input features, causing a large effect. When using the node embedding on arXiv, the GNNs still achieve improvements; it seems that input features containing the topological information still have effects on arXiv. However, when the GNNs are applied to the Products dataset, no improvements are found. All the models with Laplacian eigenvectors (except MLP with 16 layers) achieve improvements on Products, but only GCN and GAT with 4 layers improve on arXiv. This phenomenon shows that the impact of the location information described by the Laplacian eigenvectors plays a larger role in the Products dataset than in the arXiv dataset.

5. Conclusions

This study created a benchmark framework for node classification with GNNs, allowing researchers to test how the architectures and input features of various models affect the results. A k-fold model assessment was defined and applied to the small datasets. We also defined a set of model training procedures, including how to decrease the learning rate and when to terminate training. The result is a standard experimental pipeline for GNNs that helps ensure fair model comparisons. For all the models, 2 parameter budgets with different numbers of layers are used to

test whether the number of parameters affects the results. Overall, our goal in this study was to construct a benchmark to assist in testing model performance on different datasets instead of obtaining the best classification accuracy.

- We found that for graphs containing topological information, all the GNNs performed well compared with the baseline on the small datasets except for PubMed. It appears that topological information does not play an important role in improving GNN classification accuracy on PubMed.
- For the artificially generated SBMs used in social networks, we found that increasing the number of layers elevates the results, especially on CLUSTER for most models. It appears that oversmoothing is not a serious problem in node classification tasks on datasets that contain many unconnected graphs.
- To accommodate CUDA memory limitations, we first randomly sample nodes within a graph and return their induced subgraph to separate the dataset into OGBN datasets (e.g., MAG, Products and Proteins). The results show that GCN and GAT perform best on the OGBN datasets and indicate that the traditional classical models are still highly useful.
- We applied some data augmentation methods in our experiments, including node2vec embeddings and Laplacian eigenvectors. We found that the use of node2vec embeddings in MLP provides a substantial improvement on the arXiv and Products datasets and improved the GNN performance on arXiv but did not work with GNNs on the Products dataset. In contrast, the Laplacian eigenvectors did help on Products, but the improvement was limited.

5.1. Future Work

Methods such as dropedge [48], pairnorm [49] and nodenorm [50] have been proposed to solve the problems of oversmoothing and overfitting. However, these methods were tested only on small datasets in the original studies. Thus, their applicability to large datasets has not been fully verified. The experimental conditions with respect to the split among training/validation/testing and model assessment do not seem to ensure a fair comparison. Therefore, in future work, we will try to use our benchmark to test the role of the above methods in reducing the convergence speed, oversmoothing, and overfitting. When working with directed graphs, we first add edges to make them undirected, and it will be fruitful to explore how edge direction information can be considered to improve prediction performance. In addition, some datasets include some node temporal information (e.g., the year in which papers are published in arXiv and MAG); this temporal information could be included in the input features to improve the classification accuracy. To accommodate CUDA memory limitations, for some datasets, we only randomly sampled the graph nodes and returned an induced subgraph to partition the dataset. Some minibatch GNNs, especially NeighborSampling [41], GraphSAINT [26] and ClusterGCN [25], are used to perform node classification. Sometimes, these even slightly outperform the full-batch version of GNNs, which does not fit into ordinary GPU memory. Our benchmark framework is also suitable for testing these models.

Appendix A.

Table A.6: Summary of the datasets used in experiments. A split strategy, prediction task and input features are described for each dataset; more details can be found in Section 2.1.

Domain	Name	#graphs	#nodes*dim	#edges*dim	Classes
citation network datasets	Cora	1	2708*1433	5278	7
	CiteSeer	1	3327*3703	4552	6
	PubMed	1	19,717*500	44,324	3
Mathematical Modelling in social networks	PATTERN	14k	44-195*1	752~15900	2
	CLUSTER	12k	43-190*1	524~10752	6
Academic graphs	arXiv	1	169343*128	1166243(directed)	40
	MAG	1	736389*128	5416271(directed)	349
Commercial networks	Products	1	2449029*100	123718280	47
Biological networks	Proteins	1	132,534	39561252*8	2

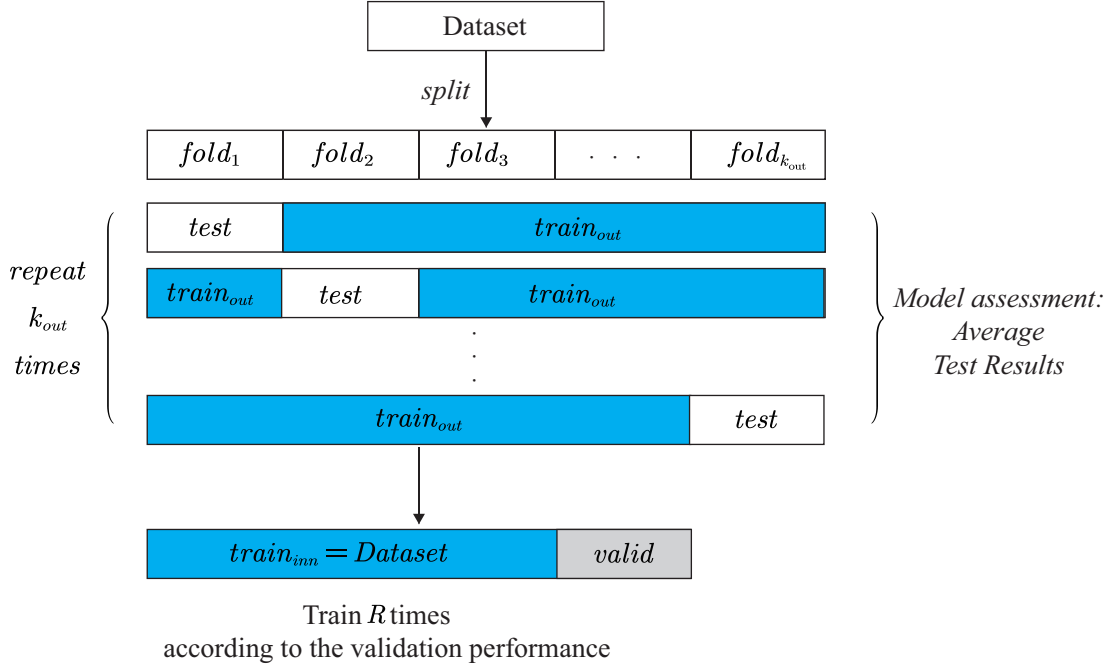


Figure A.4: The evaluation framework for small datasets

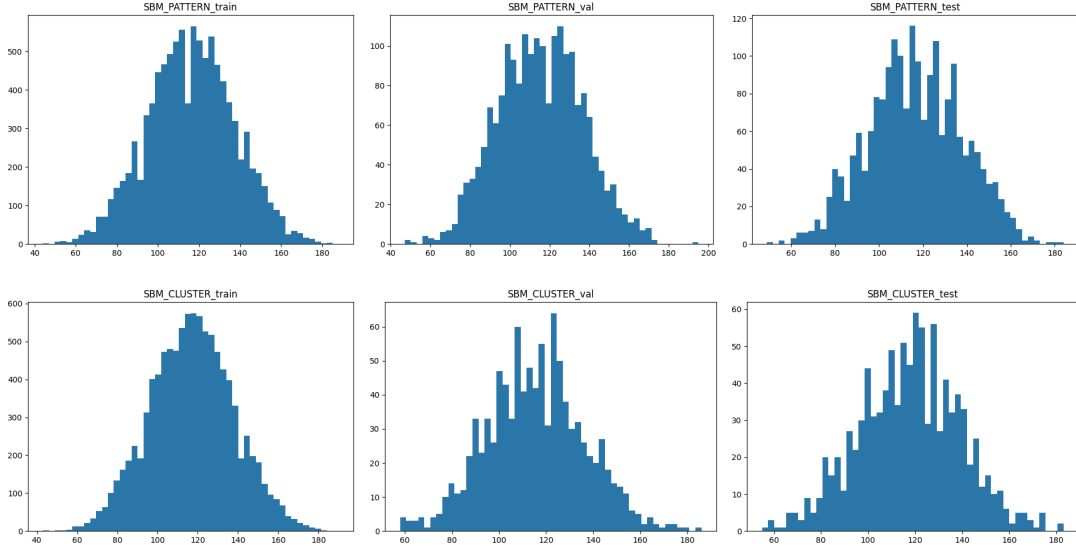


Figure A.5: A histogram of the number of nodes in each graph in the PATTERN and CLUSTER datasets

Appendix B.

GCN: Mathematically, the GCN model follows this formula:

$$h^{(l+1)} = \sigma \left(\tilde{D}^{-\frac{1}{2}} \tilde{A} \tilde{D}^{-\frac{1}{2}} h^{(l)} W^{(l)} \right) \quad (\text{B.1})$$

where $H^{(l)}$ denotes the $l^{(th)}$ layer in the network, σ is the nonlinearity, and W is the weight matrix for this layer. $\tilde{D}^{-\frac{1}{2}} \tilde{A} \tilde{D}^{-\frac{1}{2}}$ indicates a renormalization trick in which there is a self-connection to each node of the graph. Therefore,

\tilde{D} is the corresponding degree matrix of $A + I$, and $\tilde{A} = A + I$. The shape of $H^{(0)}$ is $N \times D$, where N is the number of nodes, and D is the number of input features. For better understanding, the following similar formula can also be used to describe the models.

$$h_i^{(l+1)} = \sigma \left(\sum_{j \in \mathcal{N}(i) \cup \{i\}} \frac{1}{\sqrt{\deg(i)} \cdot \sqrt{\deg(j)}} \cdot (h_j^{(l)} W^l) \right) \quad (\text{B.2})$$

where $\sqrt{\deg(i)}$ and $\sqrt{\deg(j)}$ are the degrees of nodes i and j , respectively; $\mathcal{N}(i)$ is a neighbor of node i ; and σ is the activation function; here, we used ReLU as the activation function (see Figure B.6).

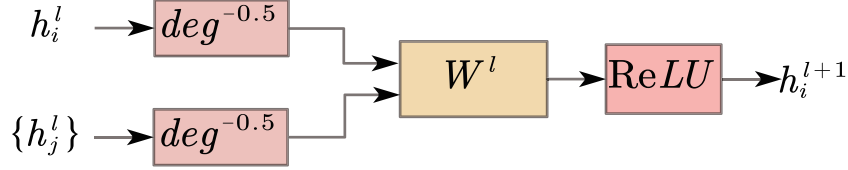


Figure B.6: GCN Layer

GraphSage: GraphSage acts as a framework for aggregating information about adjacent nodes. Under this framework, aggregate functions can be used to combine information from adjacent nodes. We then can access information from adjacent nodes when processing the current node. Finally, a norm is used for the vector that combines the information of the current node and adjacent nodes.

$$h_{\mathcal{N}(i)}^{(l+1)} = \text{aggregate}(\{h_j^l, \forall j \in \mathcal{N}(i)\}) \quad (\text{B.3})$$

$$h_i^{(l+1)} = \sigma(\text{concat}(h_i^l, h_{\mathcal{N}(i)}^{(l+1)}) \cdot W^l) \quad (\text{B.4})$$

$$h_i^{(l+1)} = \text{norm}(h_i^{(l+1)}) \quad (\text{B.5})$$

where node j is a neighbor of i , and σ is the activation function (see Figure B.7).

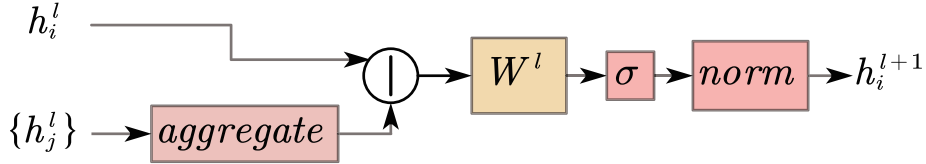


Figure B.7: GraphSage Layer

GatedGCN: In the formula, the number of input channels of \mathbf{x}_i must be less than or equal to the number of output channels. If there are fewer input channels than output channels, we first use zero vectors to complete the input channels to obtain $\mathbf{h}_i^{(0)}$ to make the input channels equal to the output channels. Θ is the learnable parameter, and e_{ij} is the edge weight. Finally, a gated recurrent unit (GRU) is used in the algorithm to implement long-term memory (see Figure B.8).

$$\mathbf{h}_i^{(0)} = \mathbf{x}_i \parallel \mathbf{0} \quad (\text{B.6})$$

$$\mathbf{m}_i^{(l+1)} = \sum_{j \in \mathcal{N}(i)} \Theta \cdot e_{ij} \cdot \mathbf{h}_j^{(l)} \quad (\text{B.7})$$

$$\mathbf{h}_i^{(l+1)} = \text{GRU}(\mathbf{m}_i^{(l+1)}, \mathbf{h}_i^{(l)}) \quad (\text{B.8})$$

Unlike the GCN, which adds the surrounding information, and GraphSAGE, which concatenates the surrounding information into its own embedding, GatedGCN uses the GRU method to collect the surrounding information and support modeling of long-term dependencies.

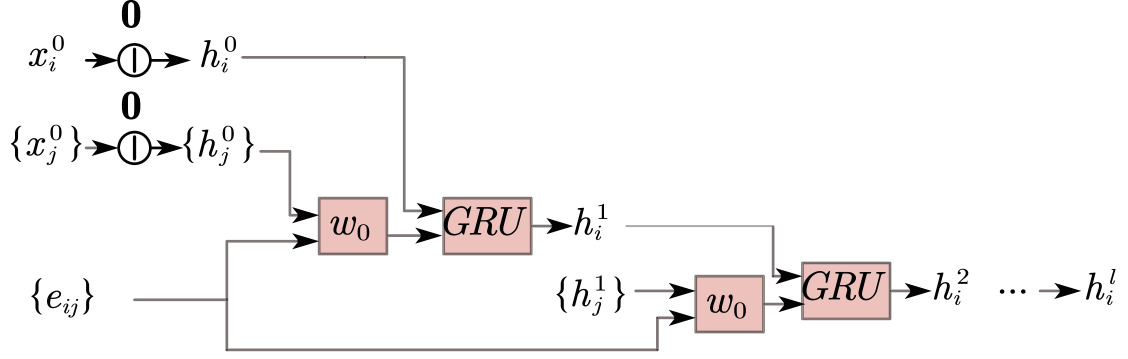


Figure B.8: GatedGCN layer

ResGatedGCN: In the ResGatedGCN formula, A^l, B^l, C^l, D^l, E^l are all learnable parameters, ε is a small fixed constant for numerical stability, and σ is the sigmoid function. In detail, the edge gates [51] can be regarded as a soft attention process, which is related to the standard sparse attention mechanism [52]. In contrast to other GNNs, the GatedGCN architecture explicitly maintains the edge features e_{ij} in each layer [53] [54] (see Figure B.9).

$$\hat{e}_{ij}^l = E^l h_i^l + B^l h_j^l + C^l e_{ij}^l \quad (\text{B.9})$$

$$e_{ij}^{l+1} = \text{ReLU}(\hat{e}_{ij}^l) \quad (\text{B.10})$$

$$h_i^{l+1} = \text{ReLU} \left(A^l h_i^l + \frac{\sum_{j \in \mathcal{N}} \sigma(\hat{e}_{ij}^l) B^l h_j^l}{\sum_{j \in \mathcal{N}} \sigma(\hat{e}_{ij}^l) + \varepsilon} \right) \quad (\text{B.11})$$

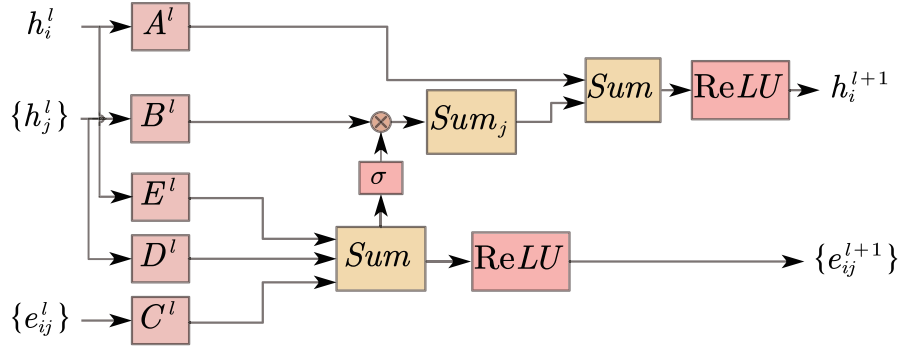


Figure B.9: ResGatedGCN layer

GAT: The core idea of the GAT is to learn the importance of neighboring nodes and then use the learned importance weight to carry out weighted summation to update a node's own embedding.

$$z_i^{(l)} = W^{(l)} h_i^{(l)} \quad (\text{B.12})$$

$$e_{ij}^{(l)} = \text{LeakyReLU}(\vec{a}^{(l)T} (z_i^{(l)} \| z_j^{(l)})) \quad (\text{B.13})$$

$$\alpha_{ij}^{(l)} = \frac{\exp(e_{ij}^{(l)})}{\sum_{k \in \mathcal{N}(i)} \exp(e_{ik}^{(l)})} \quad (\text{B.14})$$

$$h_i^{(l+1)} = \sigma \left(\sum_{j \in \mathcal{N}(i) \cup \{i\}} \alpha_{ij}^{(l)} z_j^{(l)} \right) \quad (\text{B.15})$$

where $[\]$ indicates concatenating the features of node i and node j , which have been added by the linear map of the shared parameter W . $\vec{a}^T(\cdot)$ is a learnable weight vector. A single-layer feedforward neural network is applied; then, LeakyReLU (\cdot) and softmax $_i(\cdot)$ are used to calculate the attention coefficient α_{ij}^l . Finally, the node embedding is aggregated using the learned coefficient α_{ij}^l to obtain the node embedding of the $l + 1$ layer (see Figure B.10).

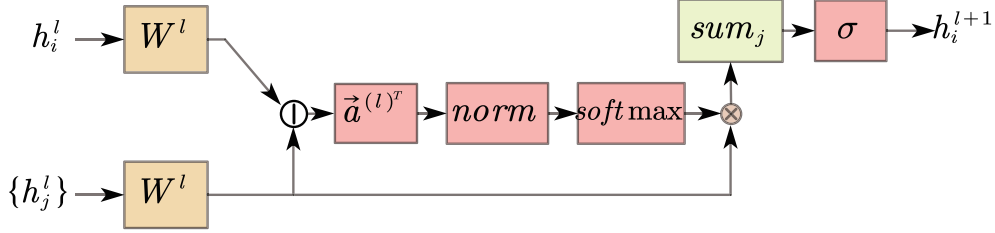


Figure B.10: GAT layer

MONET: Mixture model networks are a deep network framework run in non-Euclidean space. In the case of graphs, the node update equation is defined as follows:

$$z_i^{(l)} = W^{(l)} h_i^{(l)} \quad (\text{B.16})$$

$$h_i^{(l+1)} = \frac{1}{|\mathcal{N}(i)|} \sum_{j \in \mathcal{N}(i)} \sum_{k=1}^K \mathbf{w}_k(\mathbf{e}_{i,j}) \odot \Theta_k h_j^l + h_i^{(l)} \Theta \quad (\text{B.17})$$

$$\mathbf{w}_k(\mathbf{e}) = \exp \left(-\frac{1}{2} (\mathbf{e} - \mu_k)^\top \Sigma_k^{-1} (\mathbf{e} - \mu_k) \right) \quad (\text{B.18})$$

$$\mathbf{e} = \tanh \left(\Theta \left(\text{deg}_i^{-1/2}, \text{deg}_j^{-1/2} \right)^\top \right) \quad (\text{B.19})$$

where μ_k and Σ_k^{-1} denote the (learnable) parameters of the mean vector and diagonal covariance matrix, respectively; Θ_k and Θ are the learnable parameters; and \mathbf{e} and $\mathbf{e}_{i,j}$ are the same. The edge attributes of nodes i and j are shown in Figure B.11.

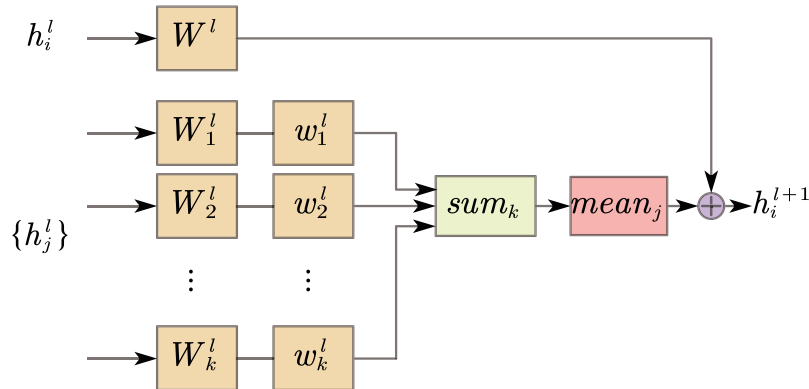


Figure B.11: Monet layer

GIN: The equations below compute the node embedding $h_i^{(l+1)}$ of layer $l + 1$ from the embeddings of layer l :

$$h_i^{(l+1)} = \text{MLP}^{(l)} \left((1 + \epsilon^{(l)}) \cdot h_i^{(l)} + \sum_{j \in N(i)} h_j^{(l)} \right) \quad (\text{B.20})$$

where l denotes the l -th layer in the network, ϵ is a learnable parameter or a fixed scalar, $N(i)$ denotes the set of neighbor indices of node i , and MLP represents the multilayer perceptron (see Figure B.12). In the first iteration, if the input features are one-hot encodings, MLP is not used before summation. For GIN, we consider the feature outputs from each layer of the network.

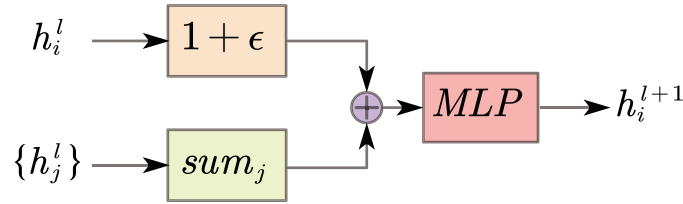


Figure B.12: GIN layer

References

- [1] W. L. Hamilton, R. Ying, J. Leskovec, Representation learning on graphs: Methods and applications, arXiv preprint arXiv:1709.05584 (2017).
- [2] S. Bhagat, G. Cormode, S. Muthukrishnan, Node classification in social networks, in: Social Network Data Analytics, Springer, 2011, pp. 115–148.
- [3] M. Zhang, Z. Cui, M. Neumann, Y. Chen, An end-to-end deep learning architecture for graph classification, in: Thirty-Second AAAI Conference on Artificial Intelligence, 2018.
- [4] Z. Ying, J. You, C. Morris, X. Ren, W. Hamilton, J. Leskovec, Hierarchical graph representation learning with differentiable pooling, in: Advances in Neural Information Processing Systems, 2018, pp. 4800–4810.
- [5] C. Cangea, P. Veličković, N. Jovanović, T. Kipf, P. Liò, Towards sparse hierarchical graph classifiers, arXiv preprint arXiv:1811.01287 (2018).
- [6] F. M. Bianchi, D. Grattarola, C. Alippi, L. Livi, Graph neural networks with convolutional arma filters, arXiv preprint arXiv:1901.01343 (2019).
- [7] L. C. Freeman, Visualizing social networks, Journal of social structure 1 (1) (2000) 4.
- [8] B. Perozzi, R. Al-Rfou, S. Skiena, Deepwalk: Online learning of social representations, in: Proceedings of the 20th ACM SIGKDD International Conference on Knowledge Discovery and Data Mining, 2014, pp. 701–710.
- [9] D. Liben-Nowell, J. Kleinberg, The link-prediction problem for social networks, Journal of the American society for information science and technology 58 (7) (2007) 1019–1031.
- [10] B. Yang, W.-t. Yih, X. He, J. Gao, L. Deng, Embedding entities and relations for learning and inference in knowledge bases, arXiv preprint arXiv:1412.6575 (2014).
- [11] T. N. Kipf, M. Welling, Semi-supervised classification with graph convolutional networks, arXiv preprint arXiv:1609.02907 (2016).
- [12] J. Zheng, Y. Wang, W. Xu, Z. Gan, P. Li, J. Lv, GSSA: Pay attention to graph feature importance for GCN via statistical self-attention, Neurocomputing 417 (2020) 458–470.
- [13] G. Zhao, P. Jia, A. Zhou, B. Zhang, InfGCN: Identifying influential nodes in complex networks with graph convolutional networks, Neurocomputing 414 (2020) 18–26. doi:10.1016/j.neucom.2020.07.028.
- [14] G. Guo, W. Yuan, Short-term traffic speed forecasting based on graph attention temporal convolutional networks, Neurocomputing 410 (2020) 387–393. doi:10.1016/j.neucom.2020.06.001.
- [15] J. Wang, J. Hu, S. Qian, Q. Fang, C. Xu, Multimodal graph convolutional networks for high quality content recognition, Neurocomputing 412 (2020) 42–51. doi:10.1016/j.neucom.2020.04.145.
- [16] J. Deng, W. Dong, R. Socher, L.-J. Li, K. Li, L. Fei-Fei, Imagenet: A large-scale hierarchical image database, in: 2009 IEEE Conference on Computer Vision and Pattern Recognition, Ieee, 2009, pp. 248–255.
- [17] W. Hu, M. Fey, M. Zitnik, Y. Dong, H. Ren, B. Liu, M. Catasta, J. Leskovec, Open graph benchmark: Datasets for machine learning on graphs, arXiv preprint arXiv:2005.00687 (2020).
- [18] T. He, Z. Zhang, H. Zhang, Z. Zhang, J. Xie, M. Li, Bag of tricks for image classification with convolutional neural networks, in: Proceedings of the IEEE Conference on Computer Vision and Pattern Recognition, 2019, pp. 558–567.
- [19] O. Shchur, M. Mumme, A. Bojchevski, S. Günnemann, Pitfalls of graph neural network evaluation, arXiv preprint arXiv:1811.05868 (2018).
- [20] F. Errica, M. Podda, D. Bacciu, A. Micheli, A fair comparison of graph neural networks for graph classification, arXiv preprint arXiv:1912.09893 (2019).
- [21] Z. Wu, S. Pan, F. Chen, G. Long, C. Zhang, S. Y. Philip, A comprehensive survey on graph neural networks, IEEE Transactions on Neural Networks and Learning Systems (2020).

- [22] V. P. Dwivedi, C. K. Joshi, T. Laurent, Y. Bengio, X. Bresson, Benchmarking graph neural networks, arXiv preprint arXiv:2003.00982 (2020).
- [23] A. Paszke, S. Gross, F. Massa, A. Lerer, J. Bradbury, G. Chanan, T. Killeen, Z. Lin, N. Gimelshein, L. Antiga, Pytorch: An imperative style, high-performance deep learning library, in: *Advances in Neural Information Processing Systems*, 2019, pp. 8026–8037.
- [24] M. Fey, J. E. Lenssen, Fast graph representation learning with PyTorch Geometric, arXiv preprint arXiv:1903.02428 (2019).
- [25] W.-L. Chiang, X. Liu, S. Si, Y. Li, S. Bengio, C.-J. Hsieh, Cluster-GCN: An efficient algorithm for training deep and large graph convolutional networks, in: *Proceedings of the 25th ACM SIGKDD International Conference on Knowledge Discovery & Data Mining*, 2019, pp. 257–266.
- [26] H. Zeng, H. Zhou, A. Srivastava, R. Kannan, V. Prasanna, Graphsaint: Graph sampling based inductive learning method, arXiv preprint arXiv:1907.04931 (2019).
- [27] P. Sen, G. Namata, M. Bilgic, L. Getoor, B. Galligher, T. Eliassi-Rad, Collective classification in network data, *AI magazine* 29 (3) (2008) 93–93.
- [28] Z. Yang, W. Cohen, R. Salakhudinov, Revisiting semi-supervised learning with graph embeddings, in: *International Conference on Machine Learning*, PMLR, 2016, pp. 40–48.
- [29] E. Abbe, Community detection and stochastic block models: Recent developments, *The Journal of Machine Learning Research* 18 (1) (2017) 6446–6531.
- [30] F. Scarselli, M. Gori, A. C. Tsoi, M. Hagenbuchner, G. Monfardini, The graph neural network model, *IEEE Transactions on Neural Networks* 20 (1) (2008) 61–80.
- [31] K. Bhatia, K. Dahiya, H. Jain, A. Mittal, Y. Prabhu, M. Varma, The extreme classification repository: Multi-label datasets and code (2016).
- [32] K. Wang, Z. Shen, C. Huang, C.-H. Wu, Y. Dong, A. Kanakia, Microsoft academic graph: When experts are not enough, *Quantitative Science Studies* 1 (1) (2020) 396–413.
- [33] D. Szklarczyk, A. L. Gable, D. Lyon, A. Junge, S. Wyder, J. Huerta-Cepas, M. Simonovic, N. T. Doncheva, J. H. Morris, P. Bork, STRING v11: Protein–protein association networks with increased coverage, supporting functional discovery in genome-wide experimental datasets, *Nucleic acids research* 47 (D1) (2019) D607–D613.
- [34] G. O. Consortium, The gene ontology resource: 20 years and still GOing strong, *Nucleic acids research* 47 (D1) (2019) D330–D338.
- [35] R. L. Murphy, B. Srinivasan, V. Rao, B. Ribeiro, Relational pooling for graph representations, arXiv preprint arXiv:1903.02541 (2019).
- [36] B. Srinivasan, B. Ribeiro, On the equivalence between node embeddings and structural graph representations, arXiv preprint arXiv:1910.00452 (2019).
- [37] M. Belkin, P. Niyogi, Laplacian eigenmaps for dimensionality reduction and data representation, *Neural computation* 15 (6) (2003) 1373–1396.
- [38] A. Grover, J. Leskovec, Node2vec: Scalable feature learning for networks, in: *Proceedings of the 22nd ACM SIGKDD International Conference on Knowledge Discovery and Data Mining*, 2016, pp. 855–864.
- [39] T. Mikolov, K. Chen, G. Corrado, J. Dean, Efficient estimation of word representations in vector space, arXiv preprint arXiv:1301.3781 (2013).
- [40] P. Veličković, G. Cucurull, A. Casanova, A. Romero, P. Lio, Y. Bengio, Graph attention networks, arXiv preprint arXiv:1710.10903 (2017).
- [41] W. Hamilton, Z. Ying, J. Leskovec, Inductive representation learning on large graphs, in: *Advances in Neural Information Processing Systems*, 2017, pp. 1024–1034.
- [42] K. Xu, W. Hu, J. Leskovec, S. Jegelka, How powerful are graph neural networks?, arXiv preprint arXiv:1810.00826 (2018).
- [43] F. Monti, D. Boscaini, J. Masci, E. Rodola, J. Svoboda, M. M. Bronstein, Geometric deep learning on graphs and manifolds using mixture model cnns, in: *Proceedings of the IEEE Conference on Computer Vision and Pattern Recognition*, 2017, pp. 5115–5124.
- [44] X. Bresson, T. Laurent, Residual gated graph convnets, arXiv preprint arXiv:1711.07553 (2017).
- [45] Y. Li, D. Tarlow, M. Brockschmidt, R. Zemel, Gated graph sequence neural networks, arXiv preprint arXiv:1511.05493 (2015).
- [46] D. P. Kingma, J. Ba, Adam: A method for stochastic optimization, arXiv preprint arXiv:1412.6980 (2014).
- [47] Q. Li, Z. Han, X.-M. Wu, Deeper insights into graph convolutional networks for semi-supervised learning, arXiv preprint arXiv:1801.07606 (2018).
- [48] Y. Rong, W. Huang, T. Xu, J. Huang, Dropedge: Towards deep graph convolutional networks on node classification, in: *International Conference on Learning Representations*, 2019.
- [49] L. Zhao, L. Akoglu, Pairnorm: Tackling oversmoothing in gnns, arXiv preprint arXiv:1909.12223 (2019).
- [50] K. Zhou, Y. Dong, W. S. Lee, B. Hooi, H. Xu, J. Feng, Effective training strategies for deep graph neural networks, arXiv preprint arXiv:2006.07107 (2020).
- [51] D. K. Duvenaud, D. Maclaurin, J. Iparraguirre, R. Bombarell, T. Hirzel, A. Aspuru-Guzik, R. P. Adams, Convolutional networks on graphs for learning molecular fingerprints, in: *Advances in Neural Information Processing Systems*, 2015, pp. 2224–2232.
- [52] D. Bahdanau, K. Cho, Y. Bengio, Neural machine translation by jointly learning to align and translate, arXiv preprint arXiv:1409.0473 (2014).
- [53] X. Bresson, T. Laurent, A two-step graph convolutional decoder for molecule generation, arXiv preprint arXiv:1906.03412 (2019).
- [54] C. K. Joshi, T. Laurent, X. Bresson, An efficient graph convolutional network technique for the travelling salesman problem, arXiv preprint arXiv:1906.01227 (2019).